PERGAMON

International Journal of Solids and Structures 39 (2002) 1361–1383

INTERNATIONAL JOURNAL OF SOLIDS and STRUCTURES

www.elsevier.com/locate/ijsolstr

Plate vibration under irregular internal supports

Y.B. Zhao [a], G.W. Wei [a,*], Y. Xiang [b]

[a] *Department of Computational Science, National University of Singapore, Level 7, Blocks S17, 3 Science Drive, Singapore 117543*

[b] *School of Engineering and Industrial Design, University of Western Sydney, Penrith South DC NSW 1797, Australia*

Received 1 November 2000

Abstract

This paper studies the problem of plate vibration under complex and irregular internal support conditions. Such a problem has its widely spread industrial applications and has not been addressed in the literature yet, partially due to the numerical difficulties. A novel computational method, discrete singular convolution (DSC), is introduced for solving this problem. The DSC algorithm exhibits controllable accuracy for approximations and shows excellent flexibility in handling complex geometries, boundary conditions and internal support conditions. Convergence and comparison studies are carried out to check the validity and accuracy of the DSC method. Case studies are considered to the combination of a few different boundary conditions and irregular internal supports. The latter are generated by using an image processing algorithm. Completely independent verifications are conducted by using the established pb-2 Ritz method, which is available for two relatively simpler support patterns. The morphology of the first few eigenmodes is found to be localized to largest support-free spatial regions.

Keywords: Square plates; Vibration analysis; Complex support; Irregular support; Discrete singular convolution; Images

1. Introduction

The analysis of plates with internal supports has been a problem of interest to engineers for over four decades. Much of the interest likely stems from potential applications of analyses to practical problems including the vibration of printed circuit boards, vibrator of cellular phones and other acoustic devices, column supported slabs, bolted aircraft and ship bodies. Indeed, most commonly used components in modern structures are the bolted, riveted or spot-welded rectangular plates which can be modeled as plates with internal supports.

Most early theoretical analyses were limited to rectangular plates with continuous internal line supports in one direction. For example, Veletsos and Newmark (1956) studied the problem of vibration of a rectangular plate simply supported at two opposite edges and continuous over rigid supports perpendicular to

* Corresponding author. Tel.: +65-874-6589; fax: +65-774-6756.
E-mail address: cscweigw@nus.edu.sg (G.W. Wei).

0020-7683/02/$ - see front matter
PII: S0020-7683(01)00241-4

those edges, using Holzer's method. A semi-graphical approach was employed by Ungar (1961) to study a similar problem. Using the dynamic edge effect approach developed by Bolotin (1961a), Bolotin (1961b) and Moskalenko and Chen (1965) analyzed plates with two and three internal line supports in one direction. Comprehensive studies were conducted by Cheung and Cheung (1971) on multi-span plates by using their finite strip method. Elishakoff and Sternberg (1979) treated similar multi-span plates in one direction, by using a modified Bolotin method.

Using the receptance method, Azimi et al. (1984) obtained closed form solutions for the vibration of simply supported multi-span rectangular plates. Mizusawa and Kajita (1984) utilized the B-spline functions in association with the Rayleigh–Ritz method to analyze free vibration of one-direction continuous plates with arbitrary boundary conditions.

Later on, there was much effort on vibration of rectangular plates with internal line supports which are continuous in two directions. Obviously, such a problem is relatively more complicated than the early ones. For example, Takahashi and Chishaki (1979) considered rectangular plates with a number of line supports in two directions by using a sine series analysis. In the framework of their finite strip method, Wu and Cheung (1974) studied free vibration of continuous rectangular plates in one or two directions by using the multi-span vibrating beam functions. Kim and Dickinson (1987) analyzed free vibration of plates with internal line supports by using a set of one-dimensional orthogonal polynomial functions as the Rayleigh–Ritz basis. Liew and Lam (1991) studied similar multi-span plates by employing the two-dimensional orthogonal polynomial functions as the Ritz trial functions. Liew et al. (1993a) investigated vibration of rectangular Mindlin plates with internal line supports in one or two directions by using the pb-2 Ritz method. In fact, their method is capable of analyzing plates with internal straight line supports in an arbitrary direction. By using appropriate polynomials, Zhou (1994) modified single-span vibrating beam functions to account for the internal line supports in one or two directions. Kong and Cheung (1995) advanced this approach by combining Zhou's trial functions with the finite layer method to study the vibration of shear-deformable plates with intermediate line supports. Li and Gorman (1993a,b) considered plates with diagonal line supports with the superposition method. The same problem was also addressed by Liew et al. (1993a) using their pb-2 Ritz method.

In practical engineering applications, many problems concern with plates having partial internal line supports. Liew and Wang (1994) studied vibration of triangular plates with partial internal curved line supports by using the pb-2 Ritz method. The point simulation approach was employed to treat the partial curved line supports in the plates.

Another class of problems which are frequently encountered in plate vibration analysis are plates with point supports. Both analytical and numerical methods are developed for treating these problems. Gorman (1981) introduced an auxiliary plate for which accurate solution is easily available to the original problem and the combined solution satisfies the governing differential equation, the boundary and support conditions. Since there is no exact solution in general, various numerical approaches, such as the finite difference method (Nishimura, 1953; Cox, 1955; Johns and Nataraja, 1972), the Rayleigh–Ritz method (Nowacki, 1953; Dowell, 1974; Narita, 1984; Laura and Cortinez, 1985), the Galerkin method (Yamada et al., 1985), the modal constraint method (Kerstens, 1979; Gorman, 1981), the finite element method (Mirza and Petyt, 1971; Rao et al., 1973; Rao et al., 1975; Utjes et al., 1984), the spline finite strip method (Fan and Cheung, 1984) and the flexibility function method (Bapat and Suryanarayan, 1989), are utilized for these problems. Recently, Liew et al. (1994a) and Kitipornchai et al. (1994) employed their pb-2 Ritz method to treat plates with point supports with success. The Lagrange multiplier approach (Kitipornchai et al., 1994) and a new constraint function approach (Liew et al., 1994a) were used to impose the point support constraints. Their method exhibits the flexibility in handling plates of arbitrary shapes with multiple point supports.

Various methods of analysis were further extended to treat plates of different shapes and thickness, with general internal supports. For example, Young and Dickinson (1993) used the Rayleigh–Ritz method with

simple polynomials as admissible functions to study the vibration of rectangular plates with straight or curved internal line supports. Liew and his co-workers used the pb-2 Rayleigh–Ritz method to study several cases, such as the vibration of triangular plates with curved internal supports (Liew, 1993), the vibration of rectangular Mindlin plates with multiple eccentric internal ring supports (Liew et al., 1993b) and the vibration of in-plane loaded plates with straight line/curved internal supports (Liew and Wang, 1993a). They also demonstrated that their method works well for the vibration of skew Mindlin plates with oblique internal line supports (Xiang et al., 1994), the vibration of skew plates with internal line supports (Liew and Wang, 1993b), the buckling and vibration of annular Mindlin plates with internal concentric ring supports subject to in-plane radial pressure (Liew et al., 1994b) and the vibration of annular sectorial Mindlin plates with internal radial line and circumferential arc supports (Liew et al., 1995). Abrate and his co-worker (Abrate, 1994, 1995, 1996; Abrate and Foster, 1995) studied the vibration of rectangular and triangular composite plates with internal supports, using the Rayleigh–Ritz method and the Lagrange multiplier technique. Lovejoy and Kapania (1996) studied the vibration of generally laminated quadrilateral, thick plates with point supports. Cheung and Zhou studied the vibration of a rectangular plate simply supported at two opposite edges with arbitrary number of elastic line supports in one way (Zhou, 1996), the eigenfrequencies of tapered rectangular plates with intermediate line supports (Cheung and Zhou, 1999a) and the vibration of rectangular composite plates with point-supports (Cheung and Zhou, 1999b). More recently, they considered the vibration of rectangular plates with elastic intermediate line-supports and edge constraints (Cheung and Zhou, 2000a), the vibration of thick, layered rectangular plates with point-supports (Cheung and Zhou, 2000b) and the vibration of symmetrically laminated rectangular plates with intermediate line supports (Cheung and Zhou, 2001). Saadatpour et al. (2000) studied the vibration of simply supported plates of general shape with internal point and line supports using the Galerkin method.

It is important to note that in most real-world structures, the support topology is both *complex* and *irregular* as required by engineering designs. For instance, commercial and military aircraft are often subjected to high levels of acoustic pressure. Therefore, they may vibrate with large amplitude displacements, i.e., with geometrical nonlinearity. Such nonlinearity may cause multi-modal interaction and lead to internal resonance. One of the most efficient methods to avoid the damage of the internal resonance is to introduce irregular internal supports. However, almost all of the literature in the field is limited to plates with simple and/or regular internal support topologies. The problem of plates with a large number of irregular supporting points seems having not been addressed in the literature, to our knowledge. Technically, it is more difficult to analyze plates with irregular internal supports. The problem is far more complicated to admit an analytical solution. Other commonly used methods encounter difficulties in one way or another. For example, it is relatively easy for the pb-2 Ritz method to treat plates with complex ring supports and any other internal support topology as long as it can be expressed as a continuous polynomial function (Liew et al., 1998). However, the efficiency of the Ritz method is dramatically reduced if the internal support topology cannot be analytically expressed. Moreover, we found that the pb-2 Ritz method, when used with the penalty approach to treat point supports, is unable to provide a convergent solution when the number of support points is relatively large. In such a case, the matrix of the eigenvalue problem becomes ill-conditioned. Another class of commonly used analysis methods in the field are the local approaches, such as finite element methods. Obviously, they are very flexible in handling the complex and irregular internal support conditions. However, the speed of convergence of conventional local methods is relatively low under complex and irregular internal support conditions due to the inherent low order approximations used. Therefore, there is a need to call for more efficient and robust methods for handling this class of engineering problems.

Discrete singular convolution (DSC) is a promising approach to resolve the aforementioned problems. The DSC concerns with the computer realization of singular convolutions (SCs) (Wei, 1999a, 2000a, 2001a). Its mathematical foundation is the theory of distributions (Schwarz, 1951) and wavelet analysis.

Numerical treatment of image processing, surface fitting and solution of differential equations is formulated via the singular kernels of the delta type. By appropriately selecting parameters of a DSC kernel, the DSC approach exhibits controllable accuracy for approximations and shows excellent flexibility in handling complex geometries, boundary and internal support conditions. It was demonstrated (Wei, 2000a) that different implementations of the DSC algorithm, such as global, local, Galerkin, collocation, and finite difference, can be deduced from a single starting point. Thus, the DSC algorithm provides a unified representation to these numerical methods. The DSC algorithm has found its success in solving the Fokker–Planck equation (Wei, 1999a, 2000a), the Schrödinger equation (Wei, 2000b), the Navier–Stokes equation for incompressible fluid flow (Wei, 2001a; Wan et al., 2001). In the context of image processing, DSC kernels were used to facilitate a new anisotropic diffusion operator for image restoration from noise corruption (Wei, 1999b). Most recently, the DSC algorithm was used to resolve a few numerically challenging problems. For example, it was utilized to integrate the sine-Gordon equation with the initial values close to a homoclinic manifold singularity (Wei, 2000c), for which conventional local methods encounter great difficulties and result in numerically induced chaos (Ablowitz et al., 1996). Another difficult example resolved by using the DSC algorithm is the integration of the Cahn–Hilliard equation in a circular domain, which is challenging because of the fourth order artificial singularity at the origin and the complex phase space geometry (Guan et al., 2001). The algorithm was utilized to facilitate a novel synchronization scheme for shock capturing (Wei, 2001b). What is the most relevant to the present work is the use of the DSC algorithm for beam and plate analysis (Wei, 2001a, 1999c,d). Previous successful examples include plate vibration under homogeneous (Zhao and Wei, submitted for publication) and mixed (Wei et al., 2001) boundary conditions, and with partial internal line supports (Wei et al., in press) and the analysis of plates with a circular shape (Wei, 2001a).

One objective of this paper is to call further attention to the study of the vibration of plates with complex and irregular internal supports. We illustrate the solution of the problem by using a few case studies. Another objective is to demonstrate the utility, robustness, and efficiency of the DSC algorithm in handling this class of problems. The validity of the DSC method for vibration analysis of plates is verified by convergence study and by a comparison with the results obtained by using the pb-2 Ritz method, which works well for a relatively simpler case. The DSC method is also tested by using irregular support points generated from random noise. The combination of a few different boundary conditions and irregular internal supports is considered in the present investigation. The topologies of irregular internal supports are generated using an image processing algorithm.

This paper is organized as follows. In Section 2, we briefly review the DSC algorithm and discuss its application to the vibration analysis of plates. Numerical results and analysis are given in Section 3. Conclusion is made in Section 4.

2. The problem and methods of solution

The problem of plate vibration with different boundary conditions and internal supports is described. For integrity and convenience, the DSC algorithm is briefly reviewed in this section. However, the reader is referred to the original work for more detailed information (Wei, 1999a, 2000a, 2001a). The implementation of the DSC algorithm to plate analysis is described.

2.1. Plate vibration

Although we limit our attention to the vibration of rectangular (classic) Kirchhoff plates with simply supported, clamped and transversely supported edges, the method can be used for many other applications

in solid mechanics. Let us consider a rectangular plate of length a, width b, thickness h, mass density ρ, modulus of elasticity E, and Poisson's ratio v. The origin of the Cartesian coordinates (x, y) is set at the lower left corner of the plate. The governing differential equation for the plate is given by (Timoshenko and Woinowsky-Krieger, 1970)

$$\frac{\partial^4 w}{\partial x^4} + 2\frac{\partial^4 w}{\partial x^2 \partial y^2} + \frac{\partial^4 w}{\partial y^4} = \frac{\rho h \omega^2}{D} w, \tag{1}$$

where $w(x, y)$ is the transverse displacement of the midsurface of the plate, $D = Eh^3/[12(1 - v^2)]$ the flexural rigidity, and ω the circular frequency. We consider one of the following three types of support conditions for each plate edge:

For simply supported edge (S)

$$w = 0, \quad -D\left(\frac{\partial^2 w}{\partial n^2} + v\frac{\partial^2 w}{\partial s^2}\right) = 0. \tag{2}$$

For clamped edge (C)

$$w = 0, \quad \frac{\partial w}{\partial n} = 0. \tag{3}$$

For transversely supported edge with nonuniform elastic rotational restraint (E)

$$w = 0, \quad -D\left(\frac{\partial^2 w}{\partial n^2} + v\frac{\partial^2 w}{\partial s^2}\right) = K(s)\frac{\partial w}{\partial n}, \tag{4}$$

where $K(s)$ is the varying elastic rotational stiffness of the plate elastic edge and n and s denote, respectively, the normal and tangential coordinates with respect to the rectangular plate edge.

2.2. Discrete singular convolution

SCs are a special class of mathematical transformations, which appear in many science and engineering problems, such as Hilbert transform, Abel transform and Radon transform. It is most convenient to discuss the SC in the context of the theory of distributions. Let T be a distribution and $\eta(t)$ be an element of the space of test functions. A SC is defined as

$$F(t) = (T * \eta)(t) = \int_{-\infty}^{\infty} T(t - x)\eta(x)\,\mathrm{d}x. \tag{5}$$

Here $T(t - x)$ is a singular kernel. Depending on the form of the kernel T, the SC is the central issue for a wide range of science and engineering problems. An important example is singular kernels of the delta type

$$T(x) = \delta^{(n)}(x) \quad (n = 0, 1, 2, \ldots). \tag{6}$$

Here, kernel $T(x) = \delta(x)$ is of particular importance for interpolation of surfaces and curves (including atomic, molecular and biological potential energy surfaces, engineering surfaces and a variety of image processing and pattern recognition problems involving low-pass filters). Higher-order kernels, $T(x) = \delta^{(n)}(x)$ $(n = 1, 2, \ldots)$, are essential for numerically solving partial differential equations (PDEs) and for image processing, noise estimation, etc. However, since these kernels are singular, they cannot be directly digitized in computers. Hence, the SC (Eq. (5)) is of little numerical merit. To avoid the difficulty of using singular expressions directly in computer, we construct sequences of approximations (T_α) to the distribution T

$$\lim_{\alpha\to\alpha_0} T_\alpha(x) \to T(x), \tag{7}$$

where α_0 is a generalized limit. Obviously, in the case of $T(x) = \delta(x)$, each element in the sequence, $T_\alpha(x)$, is a delta sequence kernel. Note that one retains the delta distribution at the limit of a delta sequence kernel. Computationally, the Fourier transform of the delta distribution is unity. Hence, it is a *universal reproducing kernel* for numerical computations and an *all pass filter* for image and signal processing. Therefore, the delta distribution can be used as a starting point for the construction of either band-limited reproducing kernels or approximate reproducing kernels. By the Heisenberg uncertainty principle, exact reproducing kernels have bad localization in the time (spatial) domain, whereas, approximate reproducing kernels can be localized in both time and frequency representations. Furthermore, with a sufficiently smooth approximation, it is useful to consider a DSC

$$F_\alpha(t) = \sum_k T_\alpha(t - x_k) f(x_k), \tag{8}$$

where $F_\alpha(t)$ is an approximation to $F(t)$ and $\{x_k\}$ is an appropriate set of discrete points on which the DSC (8) is well defined. Note that, the original test function $\eta(x)$ has been replaced by $f(x)$. The mathematical property or requirement of $f(x)$ is determined by the approximate kernel T_α. In general, the convolution is required being Lebesgue integrable.

For practical use in structure mechanics, we give several examples of delta sequence kernels, or delta kernels. A simple example is Shannon's kernel, i.e.,

$$\frac{\sin \alpha x}{\pi x}. \tag{9}$$

Other important examples include the Dirichlet kernel

$$\frac{\sin[(k+\frac{1}{2})x]}{2\pi \sin\frac{1}{2}x}, \tag{10}$$

the modified Dirichlet kernel

$$\frac{\sin[(k+\frac{1}{2})x]}{2\pi \tan\frac{1}{2}x}, \tag{11}$$

and the de la Vallée Poussin kernel

$$\frac{1}{\pi\alpha}\frac{\cos \alpha x - \cos 2\alpha x}{x^2}. \tag{12}$$

It is noted that a sequence of approximation can be improved by a regularizer (Wei, 1999a)

$$\lim_{\sigma\to\infty} R_\sigma(x) = 1. \tag{13}$$

The regularizer is designed to increase the regularity of convolution kernels. For the delta sequence, it follows from Eq. (7) that

$$\int \lim_{\alpha\to\alpha_0} T_\alpha(x) R_\sigma(x)\,\mathrm{d}x = R_\sigma(0). \tag{14}$$

Obviously, $R_\sigma(0) = 1$, is a special requirement for a *delta regularizer*. A typical delta regularizer used in the present paper is $\exp(-x^2/2\sigma^2)$. Therefore, Shannon's kernel is regularized as

$$\frac{\sin(\pi/\Delta)(x - x_k)}{(\pi/\Delta)(x - x_k)} \to \frac{\sin(\pi/\Delta)(x - x_k)}{(\pi/\Delta)(x - x_k)} \exp[-(x - x_k)^2/2\sigma^2]. \tag{15}$$

Since $\exp(-x^2/2\sigma^2)$ is a Schwartz class function, it makes the regularized kernel applicable to tempered distributions. Numerically, the regularized expressions perform much better than Shannon's kernel for being used in a local approach for solving PDEs.

Similarity, the Dirichlet kernel can be regularized as

$$\frac{\sin\left[\left(k+\frac{1}{2}\right)(x-x_k)\right]}{2\pi\sin\left[\frac{1}{2}(x-x_k)\right]} \to \frac{\sin\left[\frac{\pi}{\Delta}(x-x_k)\right]}{(2M+1)\sin\left(\frac{\pi}{\Delta}\frac{x-x_k}{2M+1}\right)}\exp[-(x-x_k)^2/2\sigma^2]. \tag{16}$$

In comparison to Shannon's kernel, the Dirichlet kernel has one more parameter M which can be optimized to achieve better results in computations. Usually, we select the value of $2M+1$ to be the grid number N for the periodic problems. Obviously, the Dirichlet kernel converts to Shannon's kernel at the limit of $M \to \infty$.

Usually, a symmetrically (or antisymmetrically) truncated DSC kernel is used to approximate the nth order derivative of a function $f(x)$ as follows

$$f^{(n)}(x) \approx \sum_{k=-M}^{M} \delta^{(n)}_{\alpha,\sigma}(x-x_k)f(x_k) \quad n=0,1,2,\ldots, \tag{17}$$

where $2M+1$ is the computational bandwidth, or effective kernel support, which is usually smaller than the whole computational domain, and $\delta^{(n)}_{\alpha,\sigma}$ is a collective symbol for the nth order derivative of any of the right-hand side of Eqs. (15) and (16).

Qian and Wei (submitted for publication) have recently provided a mathematical estimation of approximation errors. Their results provide a guide for the choice of M, σ and Δ. For example, if the L_2 error for approximation and L^2 function f is set to $10^{-\eta}$ ($\eta > 0$), the following relations are to be satisfied

$$r(\pi - B\Delta) > \sqrt{4.61\eta}, \qquad \frac{M}{r} > \sqrt{4.61\eta}, \tag{18}$$

where $r = \sigma/\Delta$ and B is the frequency bound for the function of interest. The first inequality states that for a given grid size Δ, a large r is required for approximating high frequency component of an L^2 function. The second inequality indicates that if ratio r is chosen, then an appropriate computational support can be used to ensure a given accuracy $10^{-\eta}$. This theoretical estimation is in good agreement with previous numerical tests (Wei, 2000a). The implementation of the DSC algorithm for structural analysis is described below.

2.3. Implementation of the DSC algorithm to plate analysis

For generality and simplicity, the following dimensionless parameters are introduced:

$$X = \frac{x}{a}, \quad Y = \frac{y}{b}, \quad W = \frac{w}{a}; \quad \lambda = \frac{a}{b}; \quad \Omega = \omega a^2\sqrt{\frac{\rho h}{D}}. \tag{19}$$

Accordingly, we obtain the dimensionless governing equation for the vibration analysis of a rectangular plate as:

$$\frac{\partial^4 W}{\partial X^4} + 2\lambda^2\frac{\partial^4 W}{\partial X^2\partial Y^2} + \lambda^4\frac{\partial^4 W}{\partial Y^4} = \Omega^2 W. \tag{20}$$

Consider a uniform grid having

$$0 = X_0 < X_1 < \cdots < X_{N_X} = 1,$$

and

$$0 = Y_0 < Y_1 < \cdots < Y_{N_Y} = 1.$$

To formulate the eigenvalue problem, we introduce a column vector $\mathbf{W}$ as

$$\mathbf{W} = (W_{0,0}, \ldots, W_{0,N_Y}, W_{1,0}, \ldots, W_{N_X,N_Y})^{\mathrm{T}}, \tag{21}$$

with $(N_X+1)(N_Y+1)$ entries $W_{i,j} = W(X_i, Y_j)$, $(i = 0, 1, \ldots, N_Y;\ j = 0, 1, \ldots, N_Y)$.

Let us define the $(N_q+1) \times (N_q+1)$ differentiation matrices $\mathbf{D}_q^n$ $(q = X, Y;\ n = 1, 2, \ldots)$, with their elements given by

$$\left[\mathbf{D}_q^n\right]_{i,j} = \delta_{\sigma,\Delta}^{(n)}(q_i - q_j), \quad (i, j = 0, \ldots, N_q), \tag{22}$$

where $\delta_{\sigma,\Delta}(q_i - q_j)$ is obtained from the regularized Shannon's kernel (15). However, many other DSC kernels can also be used (Wei, 2001a). The differentiation in Eq. (22) can be *analytically* carried out

$$\delta_{\sigma,\Delta}^{(n)}(q_i - q_j) = \left[\left(\frac{\mathrm{d}}{\mathrm{d}q}\right)^n \delta_{\sigma,\Delta}(q - q_j)\right]_{q=q_i} = C_m^n, \tag{23}$$

where, for a uniform grid spacing, $m = (q_i - q_j)/\Delta$. Here the matrix is banded to $i - j = m = -M, \ldots, 0, \ldots, M$. Therefore, in the matrix notation, the governing eigenvalue equation (20) is given by

$$\left(\mathbf{D}_X^4 \otimes \mathbf{I}_Y + 2\lambda^2 \mathbf{D}_X^2 \otimes \mathbf{D}_Y^2 + \lambda^4 \mathbf{I}_X \otimes \mathbf{D}_Y^4\right)\mathbf{W} = \Omega^2 \mathbf{W}, \tag{24}$$

where $\mathbf{I}_q$ is the $(N_q+1)^2$ unit matrix and $\otimes$ denotes the tensorial product. Eigenvalues can be evaluated from Eq. (24) by using a standard solver. However, appropriate boundary conditions need to be implemented before the eigenvalues can be obtained. This is described below.

We first note that boundary condition $W = 0$ is easily specified at an edge. To implement other boundary conditions, we assume, for a function f, the following relation between the inner nodes and the outer nodes on the left boundary

$$f(X_{-m}) - f(X_0) = \left(\sum_{j=0}^{J} a_m^j X_m^j\right)[(f(X_m) - f(X_0)], \tag{25}$$

where coefficients a_m^j $(m = 1, \ldots, M,\ j = 0, 1, \ldots, J)$ are to be determined by the boundary conditions. For the three types of boundary conditions described earlier, we only need to consider the zeroth order term in the power of X^j. Therefore we set $a_m^0 \equiv a_m$ and, after rearrangement, obtain

$$f(X_{-m}) = a_m f(X_m) + (1 - a_m) f(X_0), \quad m = 1, 2, \ldots, M. \tag{26}$$

According to Eq. (23), the first and the second derivatives of f on the boundary are approximated by

$$f'(X_0) = \sum_{m=-M}^{M} C_m^1 f(X_m) = \left[C_0^1 - \sum_{m=1}^{M}(1 - a_m)C_m^1\right] f(X_0) + \sum_{m=1}^{M}(1 - a_m)C_m^1 f(X_m), \tag{27}$$

and

$$f''(X_0) = \sum_{m=-M}^{M} C_m^2 f(X_m) = \left[C_0^2 + \sum_{m=1}^{M}(1 - a_m)C_m^2\right] f(X_0) + \sum_{m=1}^{M}(1 + a_m)C_m^2 f(X_m), \tag{28}$$

respectively.

For simply supported edges, the boundary conditions may be reduced to

$$f(X_0) = 0, \qquad f''(X_0) = 0. \tag{29}$$

These are satisfied by choosing $a_m = -1$, $m = 1, 2, \ldots, M$. This is the so called *anti-symmetric extension* (Wei, 1999a).

For clamped edges, the boundary conditions require

$$f(X_0) = 0, \qquad f'(X_0) = 0. \tag{30}$$

These are satisfied by $a_m = 1$, $m = 1, 2, \ldots, M$. This is the *symmetric extension* (Wei, 1999a).

For a transversely supported edge, the boundary conditions are

$$f(X_0) = 0, \qquad f''(X_0) - Kf'(X_0) = 0. \tag{31}$$

Hence, the equation is given by

$$\sum_{m=1}^{M}(1 + a_m)C_m^2 f(X_m) - K\sum_{m=1}^{M}(1 - a_m)C_m^1 f(X_m) = 0. \tag{32}$$

Further simplification of the above equation gives

$$\sum_{m=1}^{M}[(1 + a_m)C_m^2 - K(1 - a_m)C_m^1]f(X_m) = 0. \tag{33}$$

One way to satisfy Eq. (33) is to choose

$$a_m = \frac{KC_m^1 - C_m^2}{KC_m^1 + C_m^2}, \quad m = 1, 2, \ldots, M. \tag{34}$$

Expressions for the right, top and bottom boundaries can be derived in a similar way.

Further complication occurs if the coefficient K is not a constant. For example, the rotational spring coefficients of the continuous nonuniform (elastic) boundary conditions are taken as

$$K_1(Y) = K_2(Y) = K'\frac{(Y - l_1)(l_2 - Y)}{(l_2 - l_1)}, \quad (0 \leqslant l_1 < l_2 \leqslant 1), \tag{35}$$

$$K_3(X) = K_4(X) = K'\frac{(X - l_1')(l_2' - X)}{(l_2' - l_1')\lambda}, \quad (0 \leqslant l_1' < l_2' \leqslant 1), \tag{36}$$

where K' is the nondimensional spring coefficient, $K' = K_0a^3/D$, and $l_1(l_1')$, $l_2(l_2')$ are the nondimensional starting and ending points of elastic boundary, respectively. Another complication is due to the possible presence of irregular internal support condition. Hence, matrices $\mathbf{D}_X^4$, $\mathbf{D}_Y^4$, $\mathbf{D}_X^2$, $\mathbf{D}_Y^2$, $\mathbf{I}_X$ and $\mathbf{I}_Y$ become three-dimensional ones in this work and are denoted by $\mathcal{D}_X^4$, $\mathcal{D}_Y^4$, $\mathcal{D}_X^2$, $\mathcal{D}_Y^2$, $\mathcal{I}_X$ and $\mathcal{I}_Y$. The matrix elements of $\mathcal{D}_X^p$, $(p = 2, 4)$ are denoted by $d_{X,ijk}^p$, $(i, j = 0, 1, 2, \ldots, N_X;\ k = 0, 1, 2, \ldots, N_Y)$ and matrix elements of $\mathcal{I}_X$ is denoted by $\delta_{ij} \otimes 1_k$, $(k = 0, 1, 2, \ldots, N_Y)$. $\mathcal{D}_Y^p$ and $\mathcal{I}_Y$ are similarly defined by appropriately switching the roles of the subscripts.

Let us define a contractive tensor product $\dot{\otimes}$ of two three-dimension matrices $\mathscr{A}$ and $\mathscr{B}$ as the tensor product on the first two indices of $\mathscr{A}$ and $\mathscr{B}$, and contraction between the first and the third indices of the two matrices

$$(\mathscr{A}\dot{\otimes}\mathscr{B})_{ijkl} = a_{ijk}b_{kli}, \tag{37}$$

where a_{ijk} and b_{kli} are matrix elements of $\mathscr{A}$ and $\mathscr{B}$, respectively. In such a notation, Eq. (24) is modified as

$$\left[\mathcal{D}_X^4\dot{\otimes}\mathcal{I}_Y. + 2\lambda^2\mathcal{D}_X^2\dot{\otimes}\mathcal{D}_Y^2. + \lambda^4\mathcal{I}_Y\dot{\otimes}\mathcal{D}_Y^4\right]_{i(N_y+1)+k+1,\, j(N_y+1)+1+1}\mathbf{W} = \Omega^2\mathbf{W}, \tag{38}$$

where the lexicographic ordering given in Eq. (21) is used for reducing four-dimensional matrices into two-dimensional forms. Matrix elements in Eq. (38) are ready for being used in a linear equation solver

$$\mathcal{I}_X \dot{\bigotimes} \mathcal{D}_Y^4 = \left(\begin{array}{ccc|ccc|c} d^4_{Y,000} & d^4_{Y,010} & \cdots & 0 & 0 & \cdots & \\ d^4_{Y,100} & d^4_{Y,110} & \cdots & 0 & 0 & \cdots & \cdots \\ \vdots & \vdots & \ddots & \vdots & \vdots & \ddots & \\ \hline 0 & 0 & \cdots & d^4_{Y,001} & d^4_{Y,011} & \cdots & \\ 0 & 0 & \cdots & d^4_{Y,101} & d^4_{Y,111} & \cdots & \cdots \\ \vdots & \vdots & \ddots & \vdots & \vdots & \ddots & \\ \hline & \vdots & & & \vdots & & \ddots \end{array}\right)$$

$$\mathcal{D}_X^4 \dot{\bigotimes} \mathcal{I}_Y = \left(\begin{array}{ccccc|ccccc|c} d^4_{X,000} & 0 & \cdots & 0 & & d^4_{X,010} & 0 & \cdots & 0 & & \\ 0 & d^4_{X,001} & \cdots & 0 & & 0 & d^4_{X,011} & \cdots & 0 & & \cdots \\ \vdots & & \ddots & \vdots & & \vdots & & \ddots & \vdots & & \\ 0 & \cdots & \cdots & d^4_{X,00N_Y} & & 0 & \cdots & \cdots & d^4_{X,01N_Y} & & \\ \hline d^4_{X,100} & 0 & \cdots & 0 & & d^4_{X,110} & 0 & \cdots & 0 & & \\ 0 & d^4_{X,101} & \cdots & 0 & & 0 & d^4_{X,111} & \cdots & 0 & & \cdots \\ \vdots & & \ddots & \vdots & & \vdots & & \ddots & \vdots & & \\ 0 & \cdots & \cdots & d^4_{X,10N_Y} & & 0 & \cdots & \cdots & d^4_{X,11N_Y} & & \\ \hline & & \vdots & & & & & \vdots & & & \ddots \end{array}\right)$$

and

$$\mathcal{D}_x^2 \dot{\bigotimes} \mathcal{D}_y^2 = \left(\begin{array}{ccc|ccc|c} d^2_{X,000}d^2_{Y,000} & d^2_{X,000}d^2_{Y,010} & \cdots & d^2_{X,010}d^2_{Y,000} & d^2_{X,010}d^2_{Y,010} & \cdots & \\ d^2_{X,001}d^2_{Y,100} & d^2_{X,001}d^2_{Y,110} & \cdots & d^2_{X,011}d^2_{Y,100} & d^2_{X,011}d^2_{Y,110} & \cdots & \cdots \\ \vdots & \vdots & \ddots & \vdots & \vdots & \ddots & \\ \hline d^2_{X,100}d^2_{Y,001} & d^2_{X,100}d^2_{Y,011} & \cdots & d^2_{X,110}d^2_{Y,001} & d^2_{X,110}d^2_{Y,011} & \cdots & \\ d^2_{X,101}d^2_{Y,101} & d^2_{X,101}d^2_{Y,111} & \cdots & d^2_{X,111}d^2_{Y,101} & d^2_{X,111}d^2_{Y,111} & \cdots & \cdots \\ \vdots & \vdots & \ddots & \vdots & \vdots & \ddots & \\ \hline & \vdots & & & \vdots & & \ddots \end{array}\right)$$

Assume that the set of internal support points are given by $\{(X_{i'}, Y_{j'})\}$, the internal support conditions ($W_{i,j} = 0, \forall (X_i, Y_j) \in \{(X_{i'}, Y_{j'})\}$) are specified pointwisely in the matrix construction.

3. Results and discussion

The numerical algorithm proposed in this paper may be applied to square plates of various boundary conditions, including simply supported, clamped and transversely supported edges and many of their combinations. As an illustration of the DSC algorithm, square plates with uniform boundary conditions are chosen in this study.

The computational domain for a nondimensional plate is taken to be $[0,1] \times [0,1]$ in all computations. We set the DSC parameter $\sigma/\Delta = 2.5, 2.6, 2.8, 3.0, 3.2, 3.5, 3.5$ for the number of grid points $N_q = 16, 20, 24, 28, 32, 40, 67$, respectively. To be consistent with the literature, the frequency parameters reported in this paper are all scaled by a factor of π^2, i.e., Ω/π^2, where the Ω is given in Eq. (19).

The internal supports are selected including a pattern of double rhombuses, randomly distributed points, and a few images. The geometry of the double rhombuses is specified in Table 1. The randomly distributed support points are produced from a random noise generator. Twenty internal points that have absolute values larger or equal to a given value are selected from the full set of 11^2 grid (see Table 2). Six image patterns of 68^2 pixels are obtained from the Microsoft Word Clip Art pictures, and treated by using a DSC-wavelet edge detector. A summary of these images is given in Table 3. The numbers of nontrivial points of the Cherub, the ornament, the tractor, the car, the horse and the Washington are 669, 615, 715, 817, 430 and 823, respectively. In plate analysis, all support points are taken from the positions consisting the images. The coordinate values of all images and patterns used in this work are available through web download at http://www.cz3.nus.edu.sg/~guowei/research/zhaoyb.

Convergence and comparison studies are conducted in the first subsection. Some frequency parameters obtained by using the DSC algorithm are confirmed by using a completely independent method, the pb-2 Ritz method, which has been validated for plate analysis in a number of previous publications (Liew et al., 1994a; Kitipornchai et al., 1994; Liew et al., 1998).

Table 1
Convergence study of frequency parameters Ω/π^2 for SSSS and CCCC square plates with double rhombus supports

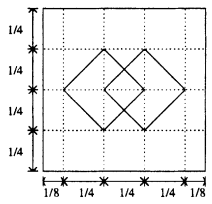

	SSSS				CCCC			
	DSC			pb-2 Ritz	DSC			pb-2 Ritz
	$N = 17$	$N = 25$	$N = 33$		$N = 17$	$N = 25$	$N = 33$	
Mode 1	15.1789	15.2325	15.2651	15.3022	21.9670	21.9946	22.0230	22.0873
Mode 2	15.2524	15.3234	15.3594	15.4493	21.9824	22.0234	22.0562	22.1116
Mode 3	15.2816	15.3422	15.3784	15.4726	22.1143	22.1510	22.1837	22.2460
Mode 4	15.3497	15.4336	15.4734	15.4775	22.1155	22.1704	22.2074	22.2629
Mode 5	21.5714	21.6346	21.7013	21.9740	29.0398	29.0894	29.1755	29.4813
Mode 6	21.6093	21.6784	21.7472	22.1864	29.0638	29.1173	29.2052	29.6120
Mode 7	27.4990	27.4657	27.4784	27.7567	36.1307	35.9141	35.8895	36.2446
Mode 8	27.7869	27.7910	27.8153	28.0800	36.7261	36.5061	36.4820	37.1527

Table 2
Convergence study of frequency parameters Ω/π^2 for SSSS and CCCC square plates with 20 random point supports

	SSSS				CCCC			
	DSC			pb-2 Ritz	DSC			pb-2 Ritz
	$N = 21$	$N = 31$	$N = 41$		$N = 21$	$N = 31$	$N = 41$	
Mode 1	13.8773	13.8325	13.8176	14.0119	14.5752	14.5165	14.4964	14.7600
Mode 2	17.4501	17.3929	17.3735	17.6255	22.7393	22.6760	22.6555	22.8537
Mode 3	19.9222	19.8300	19.7955	20.2684	24.4075	24.2807	24.2370	24.7466
Mode 4	20.4916	20.3943	20.3626	20.6783	25.5845	25.4468	25.4002	25.8383
Mode 5	23.5859	23.4864	23.4512	23.8646	26.6810	26.4528	26.3734	27.4304
Mode 6	24.0239	23.8775	23.8259	24.5362	28.6259	28.3536	28.2525	29.7271
Mode 7	26.1098	25.9175	25.8383	26.3928	32.0602	31.8502	31.7786	32.5042
Mode 8	26.2185	26.0953	26.0664	26.9833	32.5884	32.3479	32.2693	33.0650

3.1. Convergence and comparison studies

Although the validity and accuracy of the proposed DSC method were verified in the study of plate vibration under partial line supports (Wei et al., in press), the topology of previous problem is much simpler. In the present work, we further verified the reliability of the DSC algorithm for complex and irregular supports.

Convergence study is performed for simply supported and clamped square plates with a complex internal support geometry of an overlapped double rhombus pattern. Frequency parameters for the first eight modes of the two vibrating plates are presented in Table 1. Three sets of DSC grid points, varying from 17^2 to 33^2, are used to generate the frequency parameters. It is observed that, except for mode 7, the frequency parameters for the two plates increase monotonically as the number of grid points increases. When the number of DSC grid points reaches 25^2, the frequency parameters for the first eight modes in the two plates converge to a satisfactory level. Note that to ensure a certain level of reliability, all vibration frequencies presented in the case study are calculated based on a much larger number of DSC grid points (68^2).

To confirm the correctness of DSC results for thin plate analysis, we employed a completely independent approach, the pb-2 Ritz method (Wang et al., 1997), for a comparison study. The penalty approach is adopted in the pb-2 Ritz method to treat the point supports. The double rhombuses are simulated by a series of points along the rhombuses. The Ritz results in Table 1 are obtained with 20 degrees of complete two-dimensional polynomials being the Ritz trial functions. It is observed that the DSC results and the Ritz results are in good agreement in general.

We next test the reliability of the DSC algorithm for simply supported and clamped square plates with twenty randomly distributed support points. We hope that this test will act as a basis for the DSC algorithm for handling plates with irregular support conditions. Three sets of DSC grid points (21^2, 31^2 and 41^2) are used to generate the frequency parameters. The convergence speed of the first eight frequency parameters is presented in Table 2. Contrast to the vibration of plates with a double rhombus pattern, the frequency parameters for the two plates decrease monotonically as the number of grid points increases. It is seen that the DSC calculation converges well when the number of grid point reaches 31^2. For a comparison, results obtained by using the independent pb-2 Ritz method are also listed in Table 2. The Ritz results are generated with 20° of complete two-dimensional polynomials. For reliability, only the first eight modes are

Table 3
Frequency parameters Ω/π^2 for the six selected cases

		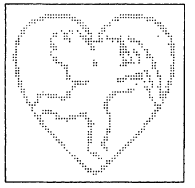	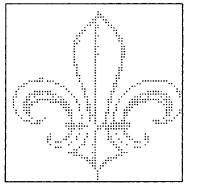	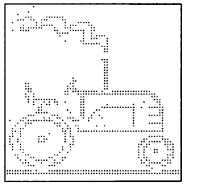	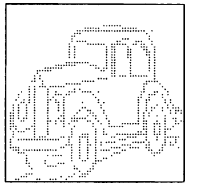	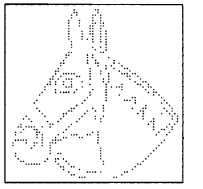	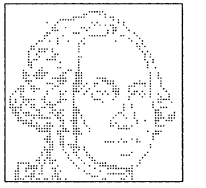
SSSS	Mode 1	23.7870	15.5935	12.8348	18.8348	14.8802	32.3169
	Mode 2	23.8699	18.3154	25.1450	37.5434	17.0974	42.6262
	Mode 3	42.9120	28.0878	25.5118	44.7970	29.5801	45.1022
	Mode 4	43.0637	32.5215	31.3190	48.9095	29.6931	45.5490
	Mode 5	54.9932	33.8671	40.5701	53.4051	32.6003	54.9473
	Mode 6	55.0451	34.2835	40.8128	55.7894	35.8931	62.7819
	Mode 7	56.7939	36.4462	46.3491	61.7358	44.0344	66.4590
	Mode 8	61.2063	45.7413	47.9205	63.6806	45.1425	71.9517
CCCC	Mode 1	34.0157	21.2111	17.4941	26.0067	20.7572	45.5249
	Mode 2	34.1405	25.2005	26.3664	48.5143	23.8770	46.5188
	Mode 3	56.2428	40.1946	31.7474	55.3379	32.8085	59.7737
	Mode 4	56.5895	40.4925	38.6097	63.6806	37.4967	64.3192
	Mode 5	56.8031	42.2503	44.7575	69.8759	38.5263	66.4694
	Mode 6	61.1953	44.5748	46.3745	71.0829	44.4396	73.0482
	Mode 7	69.7622	48.9217	49.7625	72.7538	54.6652	74.0563
	Mode 8	69.8185	56.9584	55.3288	85.0820	55.2696	92.0147
EEEE	Mode 1	27.6471	18.2417	15.2346	21.8460	17.6691	36.8347
	Mode 2	27.7388	21.3415	25.7674	42.1303	20.1875	45.5500
	Mode 3	48.0772	32.2697	28.3115	47.6566	32.6855	47.2231
	Mode 4	48.3004	35.8982	34.2065	54.8586	33.2482	50.0585
	Mode 5	56.7966	37.3695	42.5653	60.5822	33.5550	61.1172
	Mode 6	59.1281	38.5414	44.7299	61.4458	38.5358	66.4659
	Mode 7	59.1890	39.2164	46.3560	63.6806	47.5762	66.6764
	Mode 8	61.2447	49.3598	50.3239	69.5491	49.1360	77.5475

listed. Since, it is well known that the Ritz method does not work well for higher-order vibration modes. It is seen that results obtained by using both methods for the first few frequency parameters are in excellent agreement.

3.2. Case study

Having built up our confidence for using the DSC approach for plate vibration analysis with irregular support conditions, we consider vibration analysis of plates under image supports. For simplicity, the cases presented in this subsection are for square plates with three prescribed boundary conditions, i.e. simply supported at four edges (SSSS), clamped at four edges (CCCC) and transversely supported edges with nonuniform elastic rotational restraint (EEEE). The elastic support edge is considered as a simply supported edge with rotational spring constraint along the edge. The spring stiffness parameter is taken to be 100 in the present study. In fact, the geometry and support conditions resemble a notice board and/or advertisement board. As the size (number of pixels) is fixed for each image, the frequency parameters are computed by using 68^2 grid points for each image. We should point out that the pb-2 Ritz method was unable to give converged results due to the large number of internal support points.

Table 3 lists the first eight frequency parameters for each image under three different boundary conditions. For the simply supported plate (SSSS), the tractor (715 support points) has the lowest first frequency parameter (12.8348) among all images. This is because it has the largest connected free space comparing to other images. For a similar reason, the Washington (823 support points) has the highest first frequency parameter (32.3169). Although the horse has lowest number of support points (430 support points), its first frequency parameter of 14.8802 is slightly higher than that of the tractor. The same trend is observed for plates with the other two boundary conditions (i.e., CCCC and EEEE). In general, the clamped plate has the highest first frequency parameters for all six images.

The mode shapes of the simply supported plate with the six images are given in Figs. 1–6, respectively. In Fig. 1, the first vibration mode is localized to the lower right corner of the Cherub. In fact, modes 3 and 6 are also restricted to the lower right corner of the image. Modal localization phenomenon is very common in irregularly supported system since, topologically, image is essentially segmented into a few isolated regions. The largest region supports the lowest vibration mode. In fact, the size of the largest region determines the lowest value of the frequency parameter. Since the lower left corner has a size comparable to that of the lower right one, it accommodates the second vibration mode. Apparently, there are sizable indents crossing the support boundary of the heart in modes 2 and 6, which exhibit certain nonlocal nature in the mode shapes.

The ornament, as shown in Table 3, has four distinct free regions, of which the largest one is on the upper-left corner. Its modal morphology is plotted in Fig. 2. It is observed that the first vibration mode is a prime mode and is localized on the upper-left corner. Other three corners have local modes 2, 3 and 5 respectively. Modes 4 and 6 are the first excited (secondary) modes for upper-left and upper-right corners, respectively.

The morphology of the lowest few modes in Figs. 3 and 4 is also localized to largest free spatial regions. The principle for modal distribution is similar to that described in the last two paragraphs. Fig. 4 the mode distribution of the horse, has an interesting case. Its mode 5 locates essentially in the interior part of the horse. However, much of the vibration energy penetrates across the thin support boundary.

The Washington image has the most irregular distribution and the largest number of support points. As a consequence, its first frequency parameter is the highest among the six images. Fig. 6 depicts the modal distribution of the Washington. Mode 4 is of interest and is located at the forehead of the Washington.

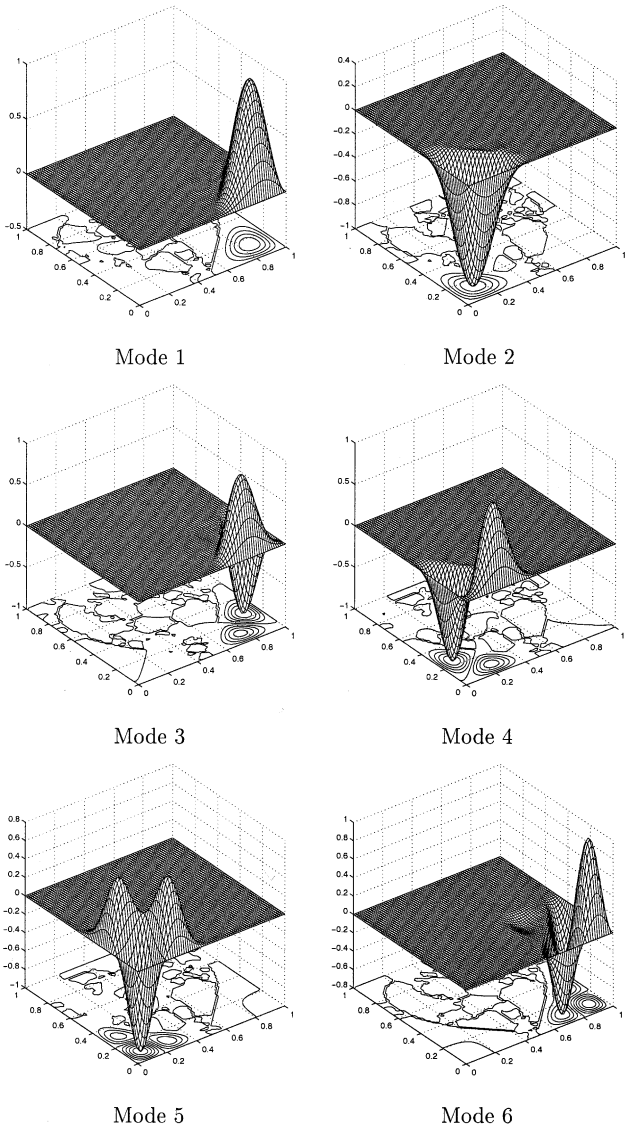

Fig. 1. Mesh and contour plots for the first six eigenmodes of the Cherub.

The localization phenomenon discussed in this work is related to engineering designs because different materials can be used in different portions of the plate so that resonance damage can be effectively avoided.

4. Conclusions

This paper addresses the issue of vibration analysis of plate with complex and irregular support conditions. The problem is of practical importance to the real-world structural designs, such as for eliminating

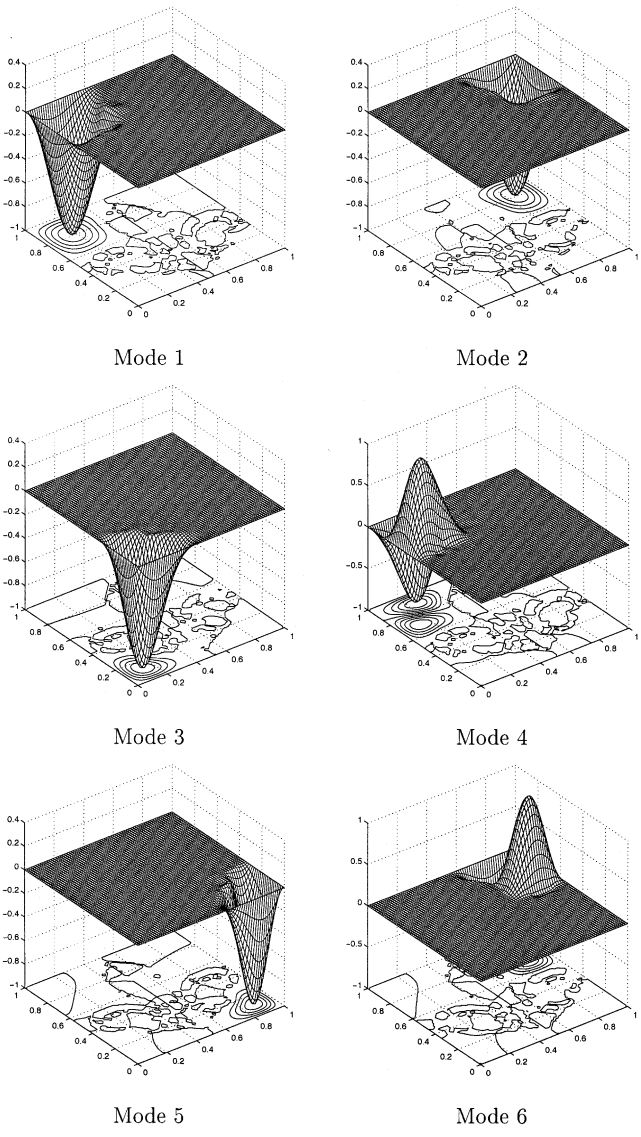

Fig. 2. Mesh and contour plots for the first six eigenmodes of the ornament.

internal resonance, and for modeling vibration of advertising broad. Numerically, this class of problems are quite challenging to conventional local methods and global methods. The local approaches might not have sufficient accuracy and the global methods might not have enough flexibility for the support conditions. For example, we found that the pb-2 Ritz method encounters difficulty in calculating frequency parameters when the number of support points is relatively large. In such a case, the solution matrix constructed by the pb-2 Ritz method becomes ill-conditioned. In the present work, we introduce a novel computational method, the DSC, for this class of problems. The DSC approach has its theoretical foundation in terms of mathematical distributions and wavelet analysis.

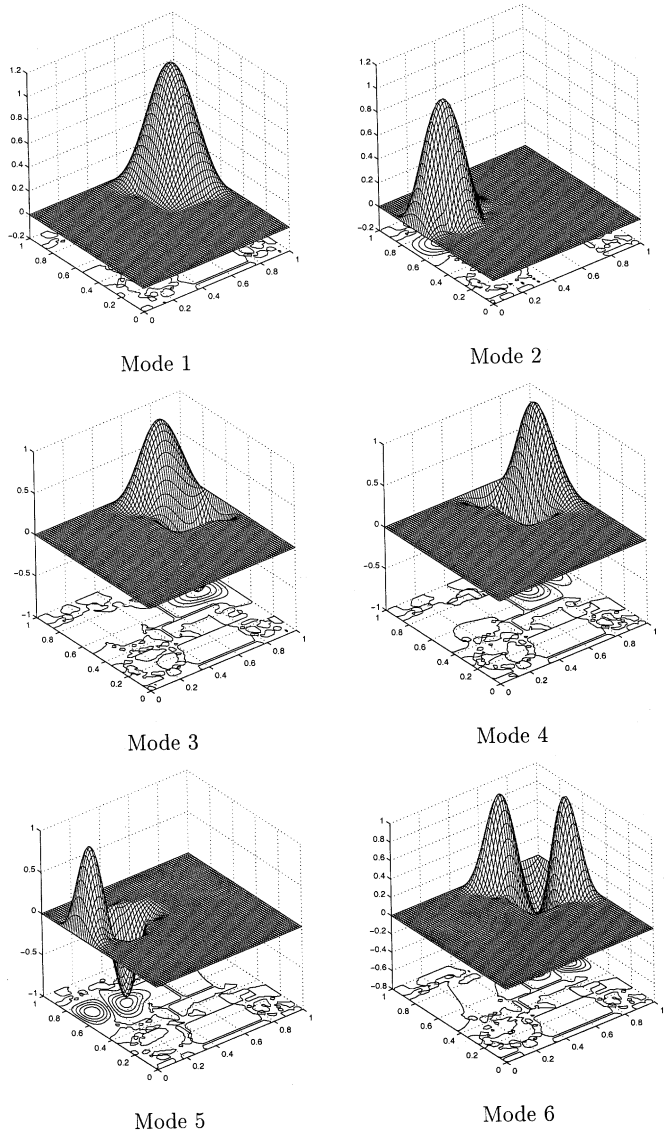

Fig. 3. Mesh and contour plots for the first six eigenmodes of the tractor.

Two special examples are designed for convergence study. The first example is a square plate with double rhombus supports. The support geometry is selected because validity of the DSC algorithm can be verified by another completely independent approach, the pb-2 Ritz method. Two boundary conditions, the SSSS and CCCC, are considered in our test calculation. In this test example, the DSC algorithm converges very well at 25^2 grid points. The results of two independent methods are consistent with each other. Our second test example is a square plate with randomly distributed support points. The number of random points is limited to twenty, a case the pb-2 Ritz method can also manage to provide reliable results. For the random nature of the problem, a reasonable estimation of frequency parameter will be sufficient. In fact, the DSC

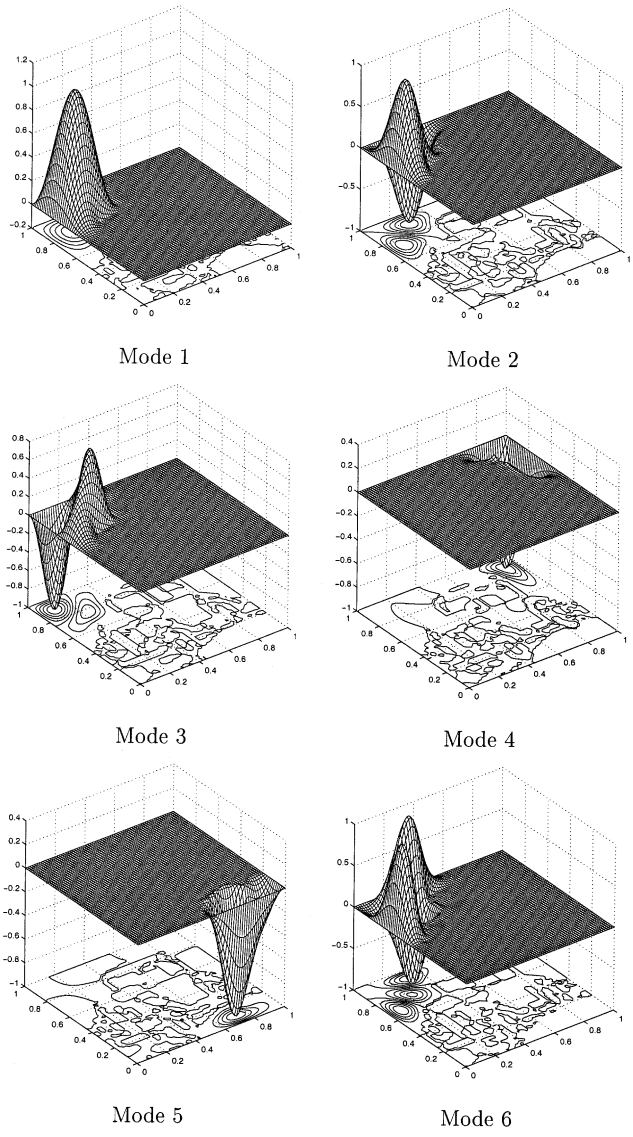

Fig. 4. Mesh and contour plots for the first six eigenmodes of the car.

readily provides excellent results at a small mesh of 21^2 for both the simply supported and clamped square plates. Once again, the DSC results are in excellent agreement with those of the pb-2 Ritz method generated by using 20 degrees of complete two-dimensional polynomials.

Six different images are selected to illustrate the possible internal support conditions one might encounter in practical applications. All images are very complicated and the pb-2 Ritz method has difficulty to produce convergent results in these cases. Three typical boundary conditions, the simply supported four edges, clamped four edges and transversely supported four edges, are considered in the present vibration

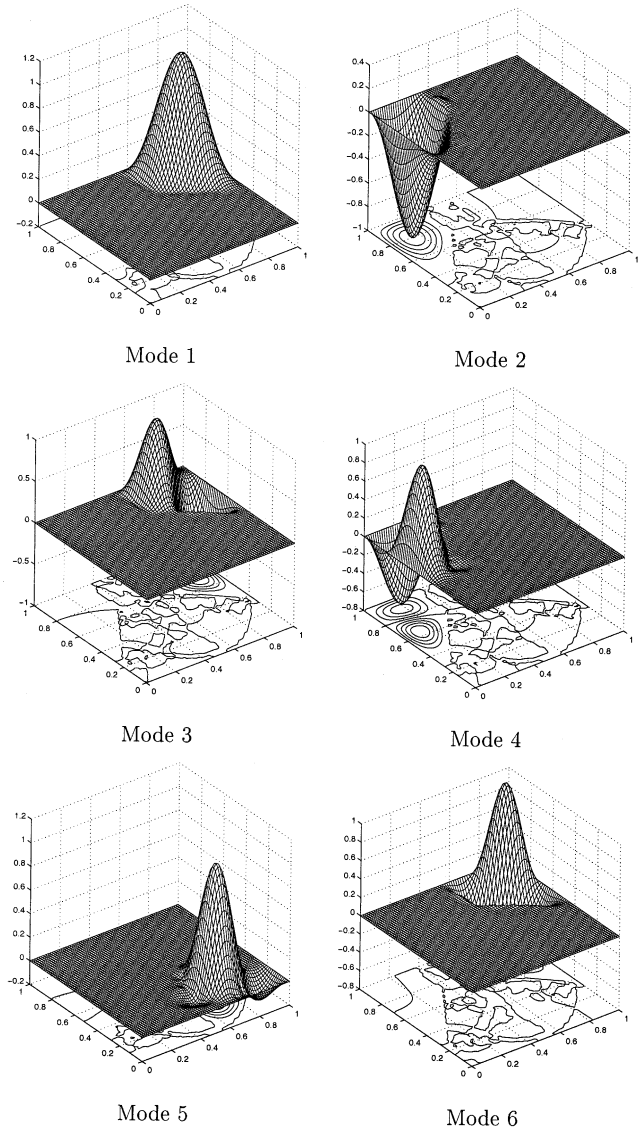

Fig. 5. Mesh and contour plots for the first six eigenmodes of the horse.

analysis. Frequency parameters of the first eight eigenmodes have been presented for these eighteen distinct cases. The modal morphology is plotted for the first six eigenmodes for plates with simply supported edges. It is observed that modal localization is a common phenomenon under complex and irregular internal support conditions. The lowest vibration energy is localized to the largest support-free spatial region. We believe that this modal localization is important to engineering design, including plate support topology optimization and material selection. The application of the present method to thick plates which involve higher order theories is under consideration.

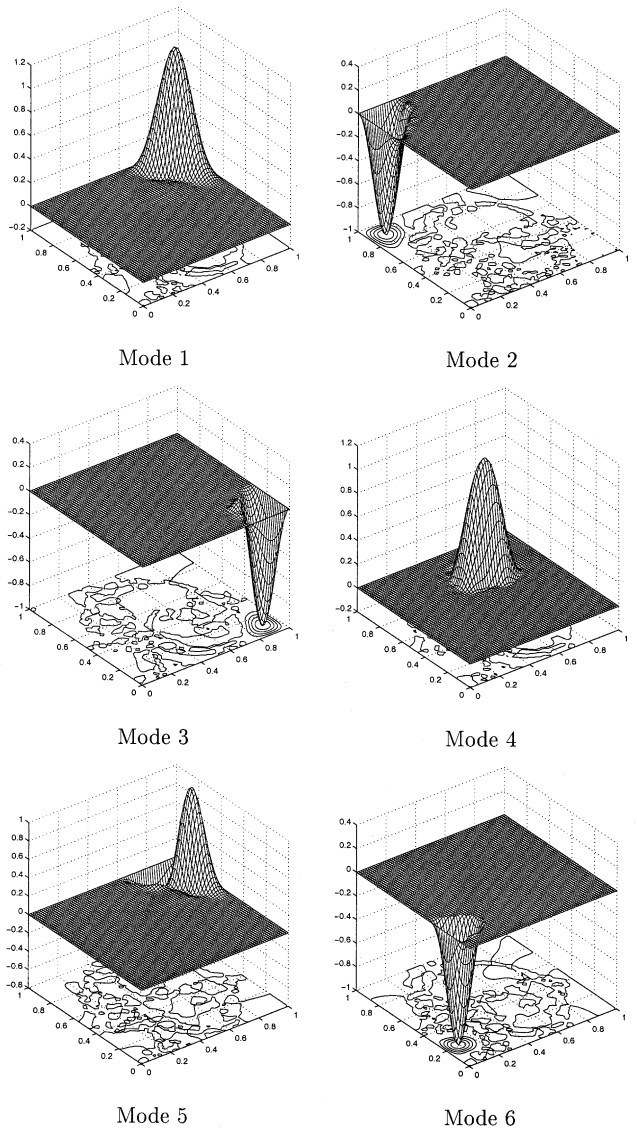

Fig. 6. Mesh and contour plots for the first six eigenmodes of the Washington.

Acknowledgements

This work was supported by the National University of Singapore and by the University of Western Sydney.

References

Ablowitz, M.J., Herbst, B.M., Schober, C., 1996. On numerical solution of the sine-Gordon equation. Journal of Computational Physics 126, 299–314.

Abrate, S., 1994. Vibration of composite plates with internal supports. International Journal of Mechanical Sciences 36 (11), 1027–1043.

Abrate, S., 1995. Vibration of point-supported rectangular composite plates. Composites Science and Technology 53, 325–332.

Abrate, S., 1996. Vibration of point supported triangular plates. Computers and Structures 58 (2), 327–336.

Abrate, S., Foster, E., 1995. Vibrations of composite plates with intermediate line supports. Journal of Sound and Vibration 179 (5), 793–815.

Azimi, S., Hamilton, J.F., Soedel, W., 1984. The receptance method applied to the free vibration of continuous rectangular plates. Journal of Sound and Vibration 93, 9–29.

Bapat, A.V., Suryanarayan, S., 1989. Free vibrations of rectangular plates with interior point supports. Journal of Sound and Vibration 134 (2), 291–313.

Bolotin, V.V., 1961a. An asymptotic method for the study of the problem of eigenvalues for rectangular regions (English edition). Problems of Continuum Mechanics, SIAM (volume dedicated to N.I. Muskhelishvili), 56–68.

Bolotin, V.V., 1961b. A generalization of the asymptotic method of the eigenvalue problems for rectangular regions. Inzhenernyi Zhurnal 3, 86–92, in Russian.

Cheung, Y.K., Cheung, M.S., 1971. Flexural vibrations of rectangular and other polygonal plates. Journal of the Engineering Mechanics Division, American Society of Civil Engineers 97, 391–411.

Cheung, Y.K., Zhou, D., 1999a. Eigenfrequencies of tapered rectangular plates with intermediate line supports. International Journal of Solids and Structures 36, 143–166.

Cheung, Y.K., Zhou, D., 1999b. Free vibration of rectangular composite plates with point-supports using static beam functions. Composite Structures 44 (2), 145–154.

Cheung, Y.K., Zhou, D., 2000a. Vibrations of rectangular plates with elastic intermediate line-supports and edge constraints. Thin-Walled Structures 37 (4), 305–331.

Cheung, Y.K., Zhou, D., 2000b. Free vibration of thick, layered rectangular plates with point supports by finite layer method. International Journal of Solids and Structures 37 (10), 1483–1499.

Cheung, Y.K., Zhou, D., 2001. Vibration analysis of symmetrically laminated rectangular plates with intermediate line supports. Computers and Structures 79, 33–41.

Cox, H.L., 1955. Vibration of a square plate, point-supported at mid-points of sides. Journal of Acoustical Society of America 27, 791–792.

Dowell, E.H., 1974. Comments on "Vibration of point supported plates". Journal of Sound and Vibration 32, 524.

Elishakoff, I., Sternberg, A., 1979. Eigenfrequencies of continuous plates with arbitrary number of equal spans. Journal of Applied Mechanics 46, 656–662.

Fan, S.C., Cheung, Y.K., 1984. Flexural free vibrations of rectangular plates with complex support conditions. Journal of Sound and Vibration 93, 81–94.

Gorman, D.J., 1981. An analytical solution for the free vibration analysis of rectangular plates resting on symmetrically distributed point supports. Journal of Sound and Vibration 79, 561–574.

Guan, S., Lai, C.-H., Wei, G.W., 2001. Fourier-Bessel characterizations of patterns in a circular domain. Physica D 151, 83–98.

Johns, D.J., Nataraja, R., 1972. Vibration of a square plate symmetrically supported at four points. Journal of Sound and Vibration 25, 75–82.

Kerstens, J.G.M., 1979. Vibration of a rectangular plate supported at an arbitrary number of points. Journal of Sound and Vibration 65, 493–504.

Kim, C.S., Dickinson, S.M., 1987. The flexural vibration of line supported rectangular plate systems. Journal of Sound and Vibration 114, 129–142.

Kitipornchai, S., Xiang, Y., Liew, K.M., 1994. Vibration of analysis of corner supported Mindlin plates of arbitrary shape using the Lagrange multiplier method. Journal of Sound and Vibration 173, 457–470.

Kong, J., Cheung, Y.K., 1995. Vibration of shear-deformable plates with intermediate line supports: a finite layer approach. Journal of Sound and Vibration 184, 639–649.

Laura, P.A.A., Cortinez, V.H., 1985. Fundamental frequency of point-supported square plates carrying concentrated masses. Journal of Sound and Vibration 100, 456–458.

Li, N., Gorman, D.J., 1993a. Free vibration analysis of rectangular plates with free edges and line support along diagonals. AIAA Journal 30 (9), 2351–2353.

Li, N., Gorman, D.J., 1993b. Free vibration analysis of simply supported rectangular plates with internal line support along diagonals. Journal of Sound and Vibration 165 (2), 361–368.

Liew, K.M., 1993. On the use of pb-2 Rayleigh–Ritz method for free flexural vibration of triangular plates with curved internal supports. Journal of Sound and Vibration 165 (2), 329–340.

Liew, K.M., Kitipornchai, S., Xiang, Y., 1995. Vibration of annular sector Mindlin plates with internal radial line and circumferential arc supports. Journal of Sound and Vibration 183 (3), 401–419.

Liew, K.M., Lam, K.Y., 1991. Vibration analysis of multi-span plates having orthogonal straight edges. Journal of Sound and Vibration 147, 255–264.

Liew, K.M., Wang, C.M., 1993a. Flexural vibration of in-plane loaded plates with straight line/curved internal supports. Journal of Vibration and Acoustics, Transactions of the ASME 115 (4), 441–447.

Liew, K.M., Wang, C.M., 1993b. Vibration studies on skew plates: treatment of internal line supports. Computers and Structures 49 (6), 941–951.

Liew, K.M., Wang, C.M., 1994. Vibration of triangular plates-point supports, mixed edges and partial internal curved supports. Journal of Sound and Vibration 172 (4), 527–537.

Liew, K.M., Wang, C.M., Xiang, Y., Kitipornchai, S., 1998. Vibration of Mindlin Plates-Programming the p-Version Ritz Method. Elsevier, Oxford.

Liew, K.M., Xiang, Y., Kitipornchai, S., 1993a. Transverse vibration of thick rectangular plates—II. Inclusion of oblique internal line supports. Computers and Structures 49, 31–58.

Liew, K.M., Xiang, Y., Kitipornchai, S., 1993b. Transverse vibration of thick rectangular plates—III. Effects of multiple eccentric internal ring supports. Computers and Structures 49, 59–67.

Liew, K.M., Xiang, Y., Kitipornchai, S., 1994a. Vibration of Mindlin plates on point supports using constraint functions. Journal of Engineering Mechanics, ASCE 120, 499–513.

Liew, K.M., Xiang, Y., Kitipornchai, S., Wang, C.M., 1994b. Buckling and vibration of annular mindlin plates with internal concentric ring supports subject to in-plane radial pressure. Journal of Sound and Vibration 177 (5), 689–707.

Lovejoy, A.E., Kapania, R.K, 1996. Free vibration of thick generally laminated quadrilateral plates with point supports. Collection of Technical Papers-AIAA/ASME/ASCE/AHS Structures, Structural Dynamics and Materials Conference, AIAA 1, 248–258.

Mirza, W.H., Petyt, M., 1971. On the vibration of point-supported plates. Journal of Sound and Vibration 15, 143–145.

Mizusawa, T., Kajita, T., 1984. Vibration of continuous skew plates. Journal of Earthquake Engineering and Structural Dynamics 12, 847–850.

Moskalenko, V.N., Chen, D.-L., 1965. On the natural vibrations of multispan plates. Prikladnaya Mekhanika 1, 59–66 (in Russian).

Narita, Y., 1984. Note on vibrations of point supported rectangular plates. Journal of Sound and Vibration 93, 593–597.

Nishimura, T., 1953. Studies on vibration problems of flat plates by means of difference calculus. Proceedings of Third Japanese National Congress of Applied Mechanics, pp. 417–420.

Nowacki, W., 1953. Vibration and buckling of rectangular plates simply-supported at the periphery and at several points inside. Archiwum Mechaniki Stosowanej 5, 437 (in Polish).

Qian, L.W., Wei, G.W., submitted for publication. A note on regularized Shannon's sampling formulae. Journal of Approximation Theory.

Rao, G.V., Amba-Rao, C.L., Murthy, T.V.K., 1975. On the fundamental frequency of point supported plates. Journal of Sound and Vibration 40, 561–562.

Rao, G.V., Raju, I.S., Amba-Rao, C.L., 1973. Vibrations of point supported plates. Journal of Sound and Vibration 29, 387–391.

Schwarz, L., 1951. Théore des Distributions. Hermann, Paris.

Saadatpour, M.M., Azhari, M., Bradford, M.A., 2000. Vibration analysis of simply supported plates of general shape with internal point and line supports using the Galerkin method. Engineering Structures 22 (9), 1180–1188.

Takahashi, K., Chishaki, T., 1979. Free vibrations of two-way continuous rectangular plates. Journal of Sound and Vibration 62, 455–459.

Timoshenko, S.P., Woinowsky-Krieger, S., 1970. Theory of Plates and Shells. McGraw-Hill, Singapore.

Ungar, E.E., 1961. Free oscillations of edge-connected simply supported plate systems. Journal of Engineering for Industry 83, 434–440.

Utjes, J.C., Laura, P.A.A., Sarmiento, G.S., Gelos, R., 1984. Vibrations of thin, elastic plates with point supports: a comparative study. Institute of Applied Mechanics Publication No. 84-26.

Veletsos, A.S., Newmark, N.M., 1956. Determination of natural frequencies of continuous plates hinged along two opposite edges. Journal of Applied Mechanics 23, 97–102.

Wan, D.C., Patnaik, B.S.V., Wei, G.W., 2001. A new benchmark quality solution for the buoyancy driven cavity by discrete singular convolution, Numerical Heat Transfer 40 (3), 199–228.

Wang, C.M., Xiang, Y., Kitipornchai, S., 1997. Optimal locations of point supports in laminated rectangular plates for maximum fundamental frequency. Structural Engineering and Mechanics 5, 691–703.

Wei, G.W., 1999a. Discrete singular convolution for the solution of the Fokker–Planck equations. Journal of Chemical Physics 110, 8930–8942.

Wei, G.W., 1999b. Generalized Perona-Malik equation for image restoration. IEEE Signal Processing Letters 6, 165–168.

Wei, G.W., 1999c. Vibration analysis by a unified computational method. Proceedings of Asia-Pacific Vibration Conference'99, 13–15 December, Singapore, pp. 755–758.

Wei, G.W., 1999d. A unified method for computational mechanics. In: Wang, C.M., Lee, K.H., Ang, K.K. (Eds.), Computational Mechanics for the Next Millennium. Elsevier, Amsterdam, pp. 1049–1054.

Wei, G.W., 2000a. A unified approach for the solution of the Fokker–Planck equations. Journal of Physics A, Mathematics and General 33, 4935–4953.

Wei, G.W., 2000b. Solving quantum eigenvalue problems by discrete singular convolution. Journal of Physics B 33, 343–352.

Wei, G.W., 2000c. Discrete singular convolution method for the sine-Gordon equation. Physica D 137, 247–259.

Wei, G.W., 2001a. A new algorithm for solving some mechanical problems. Computer Methods Applied for Mechanics and Engineering 190, 2017–2030.

Wei, G.W., 2001b. Synchronization of single-side averaged coupling and its application to shock capturing. Physical Review Letters 86, 3542–3545.

Wei, G.W., Zhao, Y.B., Xiang, Y., 2001. The determination of the natural frequencies of rectangular plates with mixed boundary conditions by discrete singular convolution. International Journal of Mechanical Sciences 43, 1731–1746.

Wei, G.W., Zhao, Y.B., Xiang, Y., in press. Vibration analysis of rectangular plates with internal supports by using discrete singular convolution. I. Theory and algorithm. International Journal of Numerical Methods in Engineering.

Wu, C.I., Cheung, Y.K., 1974. Frequency analysis of rectangular plates continuous in one or two directions. Journal of Earthquake Engineering and Structural Dynamics 3, 3–14.

Xiang, Y., Kitipornchai, S., Liew, K.M., Wang, C.M., 1994. Flexural vibration of skew Mindlin plates with oblique internal line supports. Journal of Sound and Vibration 178 (4), 535–551.

Yamada, G., Irie, T., Takahashi, T., 1985. Determination of the steady state response of a Viscoelastically point-supported rectangular plate. Journal of Sound and Vibration 102, 285–295.

Young, P.G., Dickinson, S.M., 1993. On the free flexural vibration of rectangular plate with straight or curved internal line supports. Journal of Sound and Vibration 162 (1), 123–135.

Zhao, Y.B., Wei, G.W., submitted for publication. DSC Analysis of rectangular plates with nonuniform boundary conditions. Journal of Sound and Vibration.

Zhou, D., 1994. Eigenfrequencies of line supported rectangular plates. International Journal of Solids and Structures 31, 347–358.

Zhou, D., 1996. Analytical solution of transverse vibration of a rectangular plate simply supported at two opposite edges with arbitrary number of elastic line supports in one way. Applied Mathematics and Mechanics (English Edition) 17 (8), 773–779.